ChemComm

COMMUNICATION

View Article Online
View Journal | View Issue

Cite this: *Chem. Commun.*, 2023, 59, 6040

Received 2nd April 2023,
Accepted 17th April 2023

DOI: 10.1039/d3cc01623d

rsc.li/chemcomm

Cost-effective, high-performance Ni_3Sn_4 electrocatalysts for methanol oxidation reaction in acidic environments†

Danil W. Boukhvalov,[ab] Gianluca D'Olimpio,[c] Junzhe Liu,[d] Corneliu Ghica,[e] Marian Cosmin Istrate,[e] Chia-Nung Kuo,[f] Grazia Giuseppina Politano,[g] Chin Shan Lue,[f] Piero Torelli,[h] Lixue Zhang *[d] and Antonio Politano *[c]

Methanol (CH_3OH) oxidation offers a promising avenue for transitioning to clean energy, particularly in the field of direct methanol fuel cells (DMFCs). However, the development of efficient and cost-effective catalysts for the methanol oxidation reaction (MOR) remains a critical challenge. Herein, we report the exceptional electrocatalytic activity and stability of Ni_3Sn_4 toward MOR in acidic media, achieving a performance comparable to that of commercial Pt/C catalysts. Our catalyst design incorporates Earth-abundant Ni and Sn elements, resulting in a material that is 1800 times more cost-effective than Pt/C. Density functional theory (DFT) modeling substantiates our experimental findings, shedding light on the favorable reaction mechanisms and kinetics on the Ni_3Sn_4 surface. Additionally, the as-synthesized Ni_3Sn_4 electrocatalyst demonstrates commendable durability, maintaining its electrocatalytic activity even after prolonged exposure to harsh acidic conditions.

DMFCs are attractive candidates for transportable power sources due to their superior energy density, safer storage and transportation, and ease of refuelling compared to traditional hydrogen-based fuel cells.[1] However, the widespread commercialization of DMFCs has been limited due to the lack of efficient, stable, and cost-effective catalysts for MOR.[2–4] Discovering cost-effective and stable catalysts in acidic environments is crucial for the advancement of DMFC technology.

The current state-of-the-art catalysts for MOR are platinum (Pt) and palladium (Pd), which often deliver onset potentials of about 450–550 mV and hold great potential application in DMFCs. However, the high cost of these precious metals is a major barrier to large-scale implementation of MOR catalysts for DMFCs. Many transition metal catalysts have been demonstrated to be active toward MOR in alkaline conditions, but MOR onset potentials of these catalysts are too high to be used in DMFCs.[5–7] Furthermore, methanol decomposition on transition-metal surfaces generates poisoning adsorbates (especially CO[8]), which hinder their catalytic activity. Therefore, developing transition metal-based catalysts with high MOR activity, stability in acid conditions, and superior CO tolerance is of great significance and importance.

Recently, various Ni-based electrocatalysts, including Ni oxides, Fe–Ni nanoparticles, and Ni/Al_2O_3, have demonstrated impressive MOR performance under alkaline conditions.[6,7,9,10] Nonetheless, due to Ni's tendency to dissolve in acidic environments, reports of Ni-based electrocatalysts' MOR activity in acidic media are scarce. While a Ni metal catalyst supported on partially sulfonated polyaniline has exhibited notable MOR activity and stability in acidic condition,[11] pure nickel does not perform particularly well as an MOR catalyst. That being said, Ni-based alloys, characterized by their unique electronic structures and anti-corrosion properties,[12] hold potential as catalyst candidates for MOR in acidic media.

Among the various Ni-based alloys, Ni–Sn compounds represent potential candidates, especially considering that the incorporation of Sn atoms makes CO adsorption energetically unfavorable, thus totally preventing the methanation reaction.[13] Moreover, Ni–Sn compounds are abundant and widely available, making them an attractive alternative to Pt- and Pd-based catalysts from a cost perspective.[14–16]

[a] *College of Science, Institute of Materials Physics and Chemistry, Nanjing Forestry University, Nanjing 210037, P. R. China*
[b] *Institute of Physics and Technology, Ural Federal University, Mira Str. 19, 620002 Yekaterinburg, Russia*
[c] *Department of Physical and Chemical Sciences, University of L'Aquila, via Vetoio, 67100 L'Aquila (AQ), Italy. E-mail: antonio.politano@univaq.it*
[d] *College of Chemistry and Chemical Engineering, Qingdao University, Qingdao 266071, P. R. China. E-mail: zhanglx@qdu.edu.cn*
[e] *National Institute of Materials Physics, Atomistilor 405A, 077125 Magurele, Romania*
[f] *Department of Physics, National Cheng Kung University, 1 Ta-Hsueh Road, 70101 Tainan, Taiwan*
[g] *Department of Information Engineering, Infrastructures and Sustainable Energy (DIIES), University "Mediterranea" of Reggio Calabria, Loc. Feo di Vito, 89122 Reggio Calabria, Italy*
[h] *CNR-IOM, TASC Laboratory, Area Science Park-Basovizza, 34139 Trieste, Italy*

† Electronic supplementary information (ESI) available. See DOI: https://doi.org/10.1039/d3cc01623d

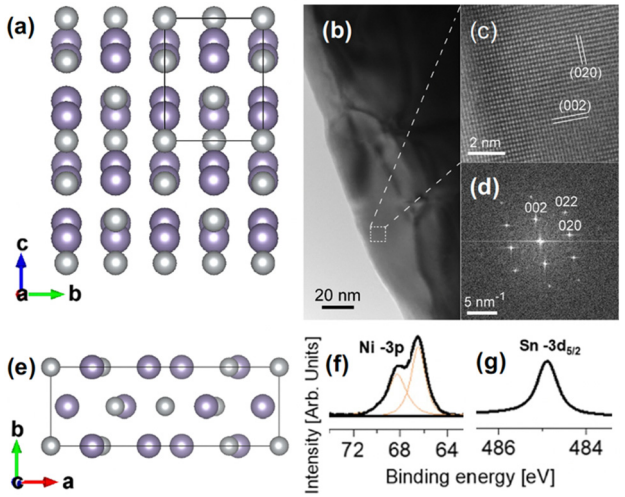

Fig. 1 (a) Top and (e) side views of the atomic structure of Ni_3Sn_4. Ni and Sn atoms are denoted by gray and purple balls, respectively. (b) TEM image of Ni_3Sn_4. Panels (c) and (d) report the HR-TEM image and the SAED pattern acquired in the region denoted by a dashed white square in panel (b). (f) Ni-3p and (g) Sn-$3d_{5/2}$ core levels of the as-cleaved Ni_3Sn_4 crystal.

Recently, Ni–Sn nanoparticles supported on carbon substrate have been tested for MOR in alkaline solution media, which showed reasonable catalytic performance.[15] However, the MOR performance of Ni–Sn compounds in acidic media has not been reported yet. Considering the potential applications in DMFCs, it is highly worthwhile to explore the MOR performance of Ni–Sn alloys with appropriate Ni ratios in acidic conditions, given their commendable corrosion resistance.[17,18]

In this work, we synthetized Ni_3Sn_4 and employed a combination of experimental and theoretical techniques to investigate its electrocatalytic properties toward MOR in acid environments. Our findings reveal the exceptional performance of Ni_3Sn_4, including its high MOR activity, stability, and superior CO tolerance, making it a promising candidate for use in DMFCs.

Single crystals of Ni_3Sn_4 were grown by the solution-growth method (see ESI,† Section S1). Ni_3Sn_4 (Fig. 1a) belongs to the $C2/m$ [no. 12] (monoclinic unit cell) space group. The X-ray diffraction (XRD in ESI,† Fig. S1 and S2), transmission electron microscopy (TEM, Fig. 1b), HR-TEM (Fig. 1c), and small-area electron diffraction (SAED) experiments (Fig. 1d) confirmed the expected Ni_3Sn_4 structure (ICSD # 105363), with lattice parameters a = 12.236 Å, b = 4.063 Å, and c = 5.224 Å. The presence of a single doublet in Ni-3p and a single component in Sn-$3d_{5/2}$ core levels further confirm the presence of a single Ni_3Sn_4 phase (see also X-ray absorption spectroscopy experiments reported in ESI†).

We measured the electrocatalytic activity of the obtained Ni_3Sn_4 toward MOR in a traditional three-electrode configuration with a scan rate of 50 mV s^{-1}. In Fig. 2a, the oxidation peak at around −0.3 V *vs.* Hg/Hg_2SO_4 is well evident in the case of the 0.5 M H_2SO_4 + 1 M CH_3OH mixture, while it is clearly absent in the case of 0.5 M H_2SO_4 only. This finding confirms the catalytic activity of Ni_3Sn_4 towards MOR. Fig. 2b shows the

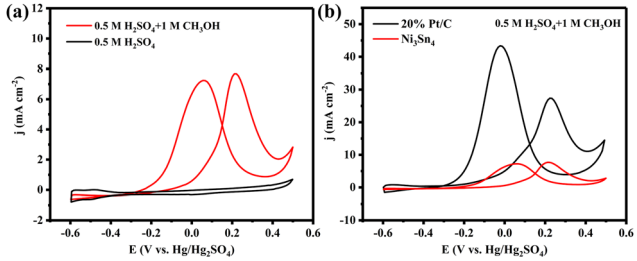

Fig. 2 (a) CV curves of Ni_3Sn_4 alloy in 0.5 M H_2SO_4 and 0.5 M H_2SO_4 + 1 M CH_3OH (scan rate of 50 mV s^{-1}), Hg/Hg_2SO_4 electrode was used as the reference electrode, graphite rod electrode was used as the counter electrode. (b) Performance comparison of Ni_3Sn_4 and commercial 20% Pt/C in 0.5 M H_2SO_4 + 1 M CH_3OH.

performance comparison between Ni_3Sn_4 and commercial 20% Pt/C in 0.5 M H_2SO_4 + 1 M CH_3OH.

Evidently, Ni_3Sn_4 exhibits a comparable onset potential to Pt/C, which is also on par with some recently reported advanced Pt-based MOR catalysts.[19] This suggests that MOR takes place more readily on Ni_3Sn_4 (Fig. 2b and Table S1, ESI†).

Taking into account the bulk structure of Ni_3Sn_4, it is not surprising that it exhibits a smaller current density (~7.8 mA cm^{-2}) compared to Pt/C (~43.0 mA cm^{-2}) (Fig. 2b). When normalizing the MOR current by the electrochemical active surface areas, the current density of Ni_3Sn_4 becomes much closer to that of Pt/C (Fig. S2, ESI†). Intriguingly, an examination of the CV curves in Fig. 2b and Fig. S2 (ESI†) reveals a larger I_f/I_b ratio (I_f and I_b are the peak currents of the forward and the backward curves, respectively) for Ni_3Sn_4 than for Pt/C, suggesting an enhanced CO tolerance for Ni_3Sn_4.[19,20] Subsequently, we performed CO stripping tests on both Ni_3Sn_4 and commercial Pt/C samples (Fig. S3, ESI†). The onset potential of CO oxidation on the Pt/C is 0.0912 V *vs.* Hg/Hg_2SO_4, while the onset potential of CO oxidation on the Ni_3Sn_4 sample is 0.0178 V *vs.* Hg/Hg_2SO_4. This result indicates a superior capability of Ni_3Sn_4 to remove adsorbed CO compared to Pt/C.

Electrochemical impedance spectroscopy (EIS) was then used to gain some insight into the MOR activity (Fig. S4, ESI†). The fitted Nyquist data shows that the charge transfer resistances (R_{ct}) of Ni_3Sn_4 and Pt/C are 6394 Ω and 3269 Ω in the mixture of 0.5 M H_2SO_4 + 1 M CH_3OH, respectively. The larger R_{ct} of Ni_3Sn_4 provides a kinetic explanation for its slightly lower MOR activity compared to Pt/C.

The durability of the Ni_3Sn_4 is also an indispensable parameter for potential applications. Firstly, the MOR process shows almost no decay after the accelerated electrochemical aging test of 1000 cycles (scan rate of 50 mV s^{-1}, Fig. 3a). Then, we carried out the chronoamperometry at 0.24 V *vs.* Hg/Hg_2SO_4 to evaluate the long-time stability. In the chronoamperometric test, Ni_3Sn_4 displays a more gradual decay process compared to Pt/C (Fig. 3b), which signifies the commendable durability of the as-prepared Ni_3Sn_4 electrocatalyst. Consequently, it can be concluded that the non-noble metal-based Ni_3Sn_4 exhibits a Pt-like catalytic performance for MOR in acidic environments,

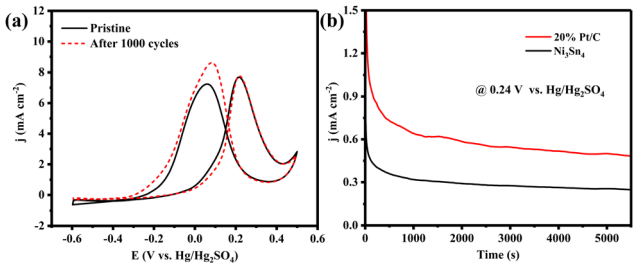

Fig. 3 (a) CV curves before and after 1000 CV scans of Ni_3Sn_4 in 0.5 M H_2SO_4 and 1 M CH_3OH solution at a scan rate of 50 mV s^{-1} (b) chronoamperometric curves of Ni_3Sn_4 and 20% Pt/C at 0.24 V (*vs.* Hg/Hg_2SO_4) in 0.5 M H_2SO_4 and 1 M CH_3OH solution.

while also offering cost reductions of up to 1800 times, thanks to the substitution of expensive Pt with an alloy composed of Earth-abundant Ni and Sn elements.

In order to reveal the pathway of MOR over the Ni_3Sn_4 surface, we performed first-principles simulations. For this purpose, we used density-functional based code Quantum Espresso.[21] For the simulation of (010) surface of Ni_3Sn_4, we used a slab of 126 atoms (see Fig. 4a). Firstly, based on recent literature on transition-metal stannides,[22,23] we checked the possible oxidation of the surface. For this purpose, physisorption and decomposition of molecular oxygen on the (010) surface of Ni_3Sn_4 were assessed. Both these processes are very energetically favourable (−1.4 and −1.1 eV per O_2). Further oxidation of whole (010) surface (Fig. 4b) is also a very favourable exothermic process, as indicated by the corresponding energy of −3.65 eV per O_2. Thus, modelling of MOR will be performed for two types of surfaces: reduced and oxidized.

In our simulations, we considered the step-by-step migration of hydrogen atoms from methanol to the substrate. The first step of the reaction displays a significant difference between reduced and oxidized Ni_3Sn_4 surfaces. On the reduced substrate, one hydrogen atom migrates from methyl group to surface Ni-atom, resulting into formation of $–OHCH_2$ group attached to two Sn atoms on the Ni_3Sn_4 surface (see Fig. 4a). In the case of oxidized substrate, the first step is the formation of the $–OCH_3$ group covalently bonded with Sn atom on substrate surface (Fig. 4b). On the other hand, on the reduced substrate, another hydrogen atom migrates from methyl group to oxygen, resulting into formation of $–OHCH_2–$ group to two Sn atoms on the substrate surface (see Fig. 4a). This difference in the reaction pathway determines the difference of the energies of the various steps of the reactions.

Calculations (Fig. 4c) indicate that, in the case of the reduced substrate, the energy cost of intermediate steps is about 1.1–1.3 eV, in qualitative agreement with the experimentally determined overpotential of about 0.9 eV (see Fig. 2 and 3). Note that the calculated energy cost is slightly larger that calculated for Pt-sites in tungsten carbide.[24] Contrarily, one of the intermediate steps of MOR over the oxidized surface corresponds to an energy cost above 2 eV, while the first step (Fig. 4b) has a very low energy barrier (0.3 eV). These values are similar to obtained in previous calculations for other substrates.[25–28]

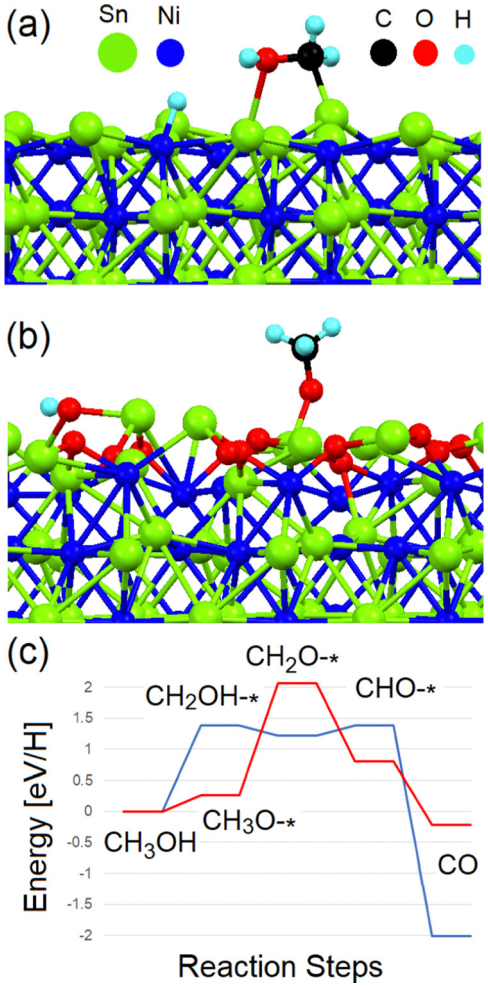

Fig. 4 (a) Optimized atomic structure of the first step of MOR on the reduced and (b) the oxidized surfaces of Ni_3Sn_4. (c) Energy diagram depicting the MOR process on both reduced (blue) and oxidized (red) surfaces of Ni_3Sn_4. The asterisk on panel (c) denotes the substrate.

Additionally, the desorption of atomic hydrogen with the formation of H_2 molecules is an exothermic process on the reduced surface (−0.3 eV), in contrast to the case of the oxidized surface. In the latter case, the removal of oxygen atoms is an endothermic process with the energy of about 0.9 eV. To merge results of the simulations with experiment, one can propose that MOR in sulphuric acid corresponds to the deoxygenation of oxidized Ni_3Sn_4, with following oxidation of methanol over reduced surface. The last step of our simulations is the evaluation of the stability of the Ni_3Sn_4 surface towards carbon monoxide poisoning. The desorption of CO from oxidized Ni_3Sn_4 surface is exothermic process with energy of −0.7 eV per CO, while an energy barrier of 0.6 eV per CO exists in the case of the reduced substrate, *i.e.*, a value more than twice smaller than in the cases of the (111) and (100) surfaces of platinum (about 1.2 and 1.4 eV per CO, respectively).[29] Thus, the desorption rate of CO is seven times larger for Ni_3Sn_4 than for platinum.

In conclusion, this study has shown that Ni_3Sn_4 exhibits a Pt-like catalytic performance for the MOR in acidic media,

demonstrating comparable activity and stability to commercial 20% Pt/C. Theoretical simulations provide insights into the pathway of MOR on the Ni_3Sn_4 surface, highlighting significant differences between reduced and oxidized surfaces. The desorption of CO from the oxidized surface is found to be seven times faster than that of platinum, indicating Ni_3Sn_4 as a potential alternative to platinum-based catalysts for MOR. Using Ni_3Sn_4 as a catalyst for MOR can significantly reduce the cost of raw materials compared to platinum-based catalysts, making it a promising candidate for use in various applications, including methanol fuel cells. The findings of this study also suggest the potential of Ni_3Sn_4 in other catalytic processes and encourage further exploration of its diverse applications.

C. G. and M. C. I. acknowledge funding through contract POC 332/390008/29.12.2020-SMIS 109522. C.-N. K. and C. S. L. acknowledge funding through the National Science and Technology Council of Taiwan under Grant No. 109-2112-M-006-013 and No. 111-2124-M-006-007. J. L. and L. Z. acknowledge funds from the National Natural Science Foundation of China (No. 22075159) and Taishan Scholars Project of Shandong Province (No. tsqn202103058).

Conflicts of interest

There are no conflicts to declare.

Notes and references

1 Z. Xia, X. Zhang, H. Sun, S. Wang and G. Sun, *Nano Energy*, 2019, **65**, 104048.
2 J. Ding, Y. Liu, A. Li, Q. Chen, P. Dong, J. Mao and X. Wei, *Chem. Commun.*, 2022, **58**, 799–802.
3 X. Gao, J. Zhang, F. Song, Q. Zhang, Y. Han and Y. Tan, *Chem. Commun.*, 2022, **58**, 4687–4699.
4 J. Luo, P. Jiang, D. Wang, X. Yuan, H. Sun, L. Gan, C. Su and Q. Zhang, *Chem. Commun.*, 2022, **58**, 4755–4758.
5 J. Wang, B. Zhang, W. Guo, L. Wang, J. Chen, H. Pan and W. Sun, *Adv. Mater.*, 2023, 2211099.
6 L. Yaqoob, T. Noor and N. Iqbal, *Int. J. Energy Res.*, 2021, **45**, 6550–6583.
7 A. Yuda, A. Ashok and A. Kumar, *Catal. Rev.*, 2022, **64**, 126–228.
8 R. Parsons and T. VanderNoot, *J. Electroanal. Chem. Interfacial*, 1988, **257**, 9–45.
9 S. L. Candelaria, N. M. Bedford, T. J. Woehl, N. S. Rentz, A. R. Showalter, S. Pylypenko, B. A. Bunker, S. Lee, B. Reinhart and Y. Ren, *ACS Catal.*, 2017, **7**, 365–379.
10 Y. Wang, W. Chen, D. Pan, Q. Xu, J. Ma, J. Zheng and R. Li, *Int. J. Electrochem. Sci.*, 2017, **12**, 2194–2206.
11 S. Das, K. Dutta and P. P. Kundu, *J. Mater. Chem. A*, 2015, **3**, 11349–11357.
12 A. Mishra, *Acta Metall. Sin. (Engl. Lett.)*, 2017, **30**, 306–318.
13 M. Fan, Y. Xu, J. Sakurai, M. Demura, T. Hirano, Y. Teraoka and A. Yoshigoe, *Int. J. Hydrogen Energy*, 2015, **40**, 12663–12673.
14 J. Li, Z. Luo, F. He, Y. Zuo, C. Zhang, J. Liu, X. Yu, R. Du, T. Zhang and M. F. Infante-Carrió, *J. Mater. Chem. A*, 2018, **6**, 22915–22924.
15 J. Li, Z. Luo, Y. Zuo, J. Liu, T. Zhang, P. Tang, J. Arbiol, J. Llorca and A. Cabot, *Appl. Catal., B*, 2018, **234**, 10–18.
16 N. A. Barakat, F. S. Al-Mubaddel, M. R. Karim, M. Alrashed and H. Y. Kim, *Int. J. Hydrogen Energy*, 2018, **43**, 21333–21344.
17 E. W. Brooman, *Met. Finish.*, 2001, **99**, 100–102.
18 C. Wan, X. Liu and J. Ye, *Surf. Coat. Technol.*, 2019, **369**, 244–251.
19 Z. Li, X. Jiang, X. Wang, J. Hu, Y. Liu, G. Fu and Y. Tang, *Appl. Catal., B*, 2020, **277**, 119135.
20 H. Sun, L. Qi, X. Jiang, G. Fu, L. Xu, D. Sun, Z. Gu and Y. Tang, *New J. Chem.*, 2017, **41**, 8812–8817.
21 P. Giannozzi, S. Baroni, N. Bonini, M. Calandra, R. Car, C. Cavazzoni, D. Ceresoli, G. L. Chiarotti, M. Cococcioni, I. Dabo, A. Dal Corso, S. de Gironcoli, S. Fabris, G. Fratesi, R. Gebauer, U. Gerstmann, C. Gougoussis, A. Kokalj, L. Michele, L. Martin-Samos, N. Marzari, F. Mauri, R. Mazzarello, S. Paolini, A. Pasquarello, L. Paulatto, C. Sbraccia, S. Scandolo, G. Sclauzero, A. P. Seitsonen, A. Smogunov, P. Umari and R. M. Wentzcovitch, *J. Phys.: Condens. Matter*, 2009, **21**, 395502.
22 D. W. Boukhvalov, A. Marchionni, J. Filippi, C. N. Kuo, J. Fujii, R. Edla, S. Nappini, G. D'Olimpio, L. Ottaviano, C. S. Lue, P. Torelli, F. Vizza and A. Politano, *J. Mater. Chem. A*, 2020, **8**, 2349–2355.
23 D. W. Boukhvalov, C.-N. Kuo, S. Nappini, A. Marchionni, G. D'Olimpio, J. Filippi, S. Mauri, P. Torelli, C. S. Lue, F. Vizza and A. Politano, *ACS Catal.*, 2021, **11**, 7311–7318.
24 T. Sheng, X. Lin, Z.-Y. Chen, P. Hu, S.-G. Sun, Y.-Q. Chu, C.-A. Ma and W.-F. Lin, *Phys. Chem. Chem. Phys.*, 2015, **17**, 25235–25243.
25 J. R. B. Gomes and J. A. N. F. Gomes, *Surf. Sci.*, 2001, **471**, 59–70.
26 S. Sakong and A. Gross, *J. Phys. Chem. A*, 2007, **111**, 8814–8822.
27 S. Liu, P. Jin, D. Zhang, C. Hao and X. Yang, *Appl. Surf. Sci.*, 2013, **265**, 443–451.
28 C.-Q. Lv, C. Liu and G.-C. Wang, *Catal. Commun.*, 2014, **45**, 83–90.
29 V. Pramhaas, M. Roiaz, N. Bosio, M. Corva, C. Rameshan, E. Vesselli, H. Grönbeck and G. Rupprechter, *ACS Catal.*, 2021, **11**, 208–214.